Ammonium ion transport by the AMT/Rh homolog LeAMT1;1

Maria Mayer, Marek Dynowski, Uwe Ludewig

Biochemical Journal Immediate Publication. Published on 27 Feb 2006 as manuscript BJ20060051

Ammonium ion transport by the AMT/Rh homolog LeAMT1;1

Maria Mayer[1], Marek Dynowski[1] & Uwe Ludewig[*]

Zentrum für Molekularbiologie der Pflanzen (ZMBP), Pflanzenphysiologie, Universität Tübingen, Auf der Morgenstelle 1, 72076 Tübingen, Germany

[1]These authors contributed equally

* Correspondence should be addressed to:

Uwe Ludewig, e-mail: uwe.ludewig@zmbp.uni-tuebingen.de

Tel.: +49 7071 2973230, Fax: +49 7071 298732

Short (page heading) title: NH_4^+ transport by AMT/Rhs

Keywords: Ammonium transport, Methylammonium, ion channel, homology modeling

Biochemical Journal Immediate Publication. Published on 27 Feb 2006 as manuscript BJ20060051

Abstract

AMT/Rh ammonium transporters/channels are identified in all domains of life and fulfill contrasting functions related either to ammonium acquisition or excretion. Based on functional and crystallographic high-resolution structural data, it was recently proposed that the bacterial AmtB is a gas channel for NH_3. Key residues, proposed to be crucial for NH_3 conduction, and the hydrophobic, but obstructed pore, were conserved in a homology model of LeAMT1;1 from tomato. Transport by LeAMT1;1 was affected by mutations that were predicted to constitute the aromatic recruitment site for NH_4^+ at the external pore entrance. Despite the structural similarities, LeAMT1;1 was shown to transport only the ion; each transported ^{14}C-MeA molecule carried a single, positive elementary charge. Similarly, NH_4^+ (or H^+/NH_3) was transported, but NH_3 conduction was excluded. It is concluded that related proteins and a similar molecular architecture can apparently support contrasting transport mechanisms.

Introduction

There is an ongoing debate as to whether some or all AMT/Rh proteins function as NH_3 channels or as NH_4^+ transporters [1]. Based on the recently obtained high-resolution structure of a bacterial homolog, AmtB from *E.coli*, a channel-like transport of NH_3 in AMT/Rh proteins has been proposed [2, 3]. Ammonium-mediated vesicular alkalinization by reconstituted AmtB [2] and studies with bacterial strains compromised in ammonium assimilation and transport are in accordance with NH_3 transport [4]. However, mechanistic interpretations from a static structure should be taken with care. Though probably within the rage of experimental error, some MeA accumulation by AmtB was detected, which was only to be expected if AmtB transports NH_4^+. MeA accumulation would be also expected if, hypothetically, the ion occasionally "slipped" through the channel/transporter [4]. Additional *in vitro* and *in vivo* experiments, including flux measurements against ammonia gradients and/or current recordings, are required to establish the NH_3 transport mechanism in AmtB. According to its transcriptional and post-transcriptional regulation, the physiological role of AmtB appears to be the uptake of ammonium under low ammonium concentrations, but the NH_3 gradient is unfavorable for uptake under most conditions [4].

The transport mechanism proposed for AMT/Rh proteins from the X-ray structures involves NH_4^+ recruitment at the external pore mouth close to the aromatic residues F103, F107 and W148, de-protonation and conduction as NH_3 [2, 3]. Hallmarks of the AMT/Rh family are

two histidines that line the central hydrophobic pore. It has been proposed that NH_4^+ cannot pass these histidines and thus no NH_4^+ transport and no ionic currents would be expected in AmtB. An electroneutral NH_3 transport by AMT/Rh homologs is compatible with our results on human RhBG and RhCG. The studies suggest that ammonium transport by these proteins is electroneutral when heterologously expressed in oocytes and yeast [7, 8], in accordance with results from other groups [9].

In contrast, specific, saturable, voltage-dependent, pH_o-independent NH_4^+ and MeA^+ currents have been recorded from two tomato AMT protein homologs expressed in oocytes [5, 6]. There is little doubt that ammonium uptake in plants is at least partially as NH_4^+, since electrogenic ammonium transport in plants is well established [1]. Ionic currents are in conflict with the proposed NH_3 channel mechanism in AMT/Rhs, but NH_4^+ currents might represent an ion "slippage", while the major transport form is NH_3. It has not been tested if NH_3 is transported through LeAMT1;1.

The surprising similarity of a LeAMT1;1 homology model to AmtB triggered a further analysis of NH_4^+ and MeA^+ currents by LeAMT1;1. While NH_4^+ and MeA^+ currents were recorded, no slippery gas (NH_3) transport was detected. It was additionally found that an aromatic residue at the outer pore mouth is involved in high affinity recruitment of NH_4^+. LeAMT1;1 may thus either function as a NH_4^+ channel (or "uniporter"), or physiologically equivalent, as NH_3/H^+ co-transporter.

Experimental

Plasmid constructs, preparation and injection of oocytes- The plasmid pOO2-*LeAMT1;1* and oocyte handling have been described in previous studies [5, 7]. Mutations were introduced into LeAMT1;1 by using the Quickchange method from Stratagene and the complete coding region was verified by sequencing.

Electrophysiological measurements & radiotracer uptake & Intracellular pH changes (pH_i) Recordings were performed as described [7]. Means ± SEM are given. There was no special selection applied, but studies on ammonium transport in oocytes may be hampered by endogeous ion channels that are activated by high ammonium such as 10 mM [10, 11]. Currents from oocytes used in this study were insensitive to ammonium and methylammonium (MeA) at concentrations of 1 mM or 10 mM, respectively [5, 12] and care was taken to verify that these endogenous ammonium-inducible currents were not present in the oocyte batches used. Oocytes used in our laboratory had a background conductance of $\leq$0.9 μS (between 0 mV and –100mV) and background currents as low as ~-80 nA at –140

mV. This background current is about half of the endogenous current from oocytes used in the laboratories that have recorded and investigated NH_4^+ induced currents [11, 13]. Interestingly, seasonal variations were reported for the endogenous amine-inducible current [11]. Although activation of such endgenous oocyte currents at lower ammonium concentrations has been reported [13], we and others observed that ionic currents from oocytes are insensitive to ammonium at $\leq$ 1 mM at physiological pH [5-7, 12, 14] (*and data not shown*). Although the nature of this discrepancy and the natural variance in oocyte currents is unclear, *Xenopus* oocytes with reduced or absent endogenous MeA^+ and NH_4^+-currents have the great advantage that measurements on ammonium transport can be performed with minimal contamination from the endogenous ammonium-induced currents. The absence of endogenous MeA^+ and NH_4^+-currents in oocytes used in this study demands that internal pH_i will respond differently to ammonium than in previous studies on oocytes with large NH_4^+-currents (Fig.5). Oocytes expressing large endogenous ammonium-activated currents had been reported to acidify slowly when measured with pH-sensitive electrodes [11, 13]. As the NH_4^+-conductance was absent in the oocytes used in our study, native oocytes alkalinized upon addition of 10 mM ammonium (Fig.5).

In the cases where currents "induced by ammonium" are given; these were obtained by subtracting the current in the absence of ammonium (background) from the current in the presence of ammonium at each voltage. NH_3 and NH_4^+ concentrations were determined from total ammonium concentrations using the Henderson-Hasselbach equation: $\log_{10}[NH_3]/[NH_4^+] = pH - 9.25$. The $pK_a = 10.66$ was used for calculations involving MeA (CH_3-NH_3^+/CH_3-NH_2). The concentration dependence of currents/uptakes were fitted using the following equation: $I=I_{max}/(1+K_m/c)$, where I_{max} is the maximal current at saturating concentration, K_m is the substrate concentration permitting half-maximal currents, and c is the experimentally used concentration. ^{14}C-MeA uptake was done as in [7].

Intracellular pH changes (pH_i) - were monitored using the pH-sensitive dye 2',7'-bis-(carboxyethyl)-5(6)-carboxyfluorescein (BCECF) and were calibrated as described [7]. Briefly, oocytes were incubated in uptake buffer (ND96, containing 5 μM BCECF-AM, from a 50 mM stock in DMSO) for 30 min protected from light. Fluorescence was monitored using an inverted Leica fluorescence microscope at maximal rate (5 sec) using a spinning wheel system with excitation at 410$\pm$30 and 470$\pm$20 nm and emission at 535$\pm$20 nm of BCECF-loaded oocytes placed in a recording chamber and superfused with the standard solution ($\pm$ NH_4Cl). In some experiments, oocytes were voltage clamped during fluorescence recording.

Homology modeling-The primary sequence of LeAMT1;1 was aligned with AmtB using ClustalW, followed by manual inspection of functionally important residues. The alignment was identical to the alignment in Khademi *et al*. (2004) for the first transmembrane helix (see supplementary figure). Structural fitting was done using MODELLER 7v7 (available at http://salilab.org/modeller/), a well-established structure prediction program [15]. The structures were evaluated using the WHATIF program (http://biotech.ebi.ac.uk:8400/) and Procheck (http://www.biochem.ucl.ac.uk/~roman/procheck/procheck.html). The LeAMT1;1 model used had 90.5% residues in the most favored regions in a Ramachandran plot (compared to 92.7% in the AmtB structure). Only 9 amino acids were identified that had "bad" stereochemistry. All of these were located outside of the core structure of the transmembrane helices. Further evaluation was done by energy minimization of the monomers of AmtB (PDB accession code: 1U7G) and the LeAMT1;1 model for 10 psec using NAMD2.5 (http://www.ks.uiuc.edu/Research/namd/), using the Amber7 force field. The stability of the structure was used as a measure for the quality and was assessed by measuring the RMSD between backbone residues of the structures. Minor attention was given to reconstruction of loops, as these are expected to minimally influence the core structure and transport mechanism. The pore diameter was accessed using the program HOLE2 (http://d2o.biop.ox.ac.uk:38080//; [16]). Monomeric bovine AQP1 (PDB accession code: 1J4N) was analyzed in parallel.

Expression in yeast –The open reading frames of LeAMT1;1 and a translational LeAMT1;1-GFP fusion were cloned into plasmid pDR196 and heat shock-transfected in the *ura*$^-$ *Saccharomyces cerevisiae* wild type strain (23344c) or the ammonium transporter defective yeast strain (31019b; *Δmep1;2;3*) [17]. The nitrogen deficient growth medium for strain 31019b was YNB (Difco), supplemented with 3% glucose and appropriate NH_4Cl concentrations. The media was adjusted to pH 5.5 using 50 mM 2-[N-morpholino]ethanesulfonic acid (MES). The MeA toxicity medium contained YNB, 3% glucose, 0.1% arginine and 125 mM MeA. Growth of yeast was not affected by expression of the different constructs under non-seletive conditions.

Results

Homology model of LeAMT1;1

To identify the molecular determinants for differences in the transport mechanism between AMT/Rh homologs, a homology model of LeAMT1;1 with AmtB (PDB code 1U7G) as template was constructed. Both proteins are 25% identical and 44% similar within the protein

core (excluding the N- and-C-terminus). The most stable model (see methods) was obtained by using a slightly modified alignment from that published by Khademi *et al.*, which is given as a supplementary figure and only differs in the first transmembrane region. A ribbon representation of the structural backbone of AmtB and the model of LeAMT1;1 is shown in Fig.1A,B. Major deviations are seen in extrahelical loops, consistent with the low similarity in these regions. The model was less stable than AmtB after a minimization for 10 ps, which reduces "bad" contacts within the protein (Fig.1C). Three monomers preferably assembled in a trimeric form (Fig.1E).

AmtB does not form an "open" channel-like structure as, e.g. aquaporin channels. Several aquaporins transport ammonia in addition to water [18, 19], which justifies the comparison between these protein classes. The substrate pore of aquaporin monomers is illustrated for bovine AQP1 (PDB code:1J4N)[20] using the program HOLE2, a program that identifies putative ionic and solute pores in proteins based on the van der Waals radii of amino acid residues close to the pore [16]. The AQP1 pore constriction does not go below 0.8 A (Fig.1D) [20], but the solute pathway in AmtB is blocked by residues F107 and F215 and partially by residue F31 (Fig.1C,F). In accordance with this, preliminary comparative steered molecular dynamics studies did reveal solute flux in aquaporins, but not in AmtB (*unpublished observation*). The fundamental difference appears important, since the proposed channel-like mechanism was recently illustrated by a misleading "open-pore" cartoon-like model [21]. At least minimal conformational changes are necessary to obtain a channel-like open pore structure. Another possibility is that transport-cycle dependent conformational changes are involved in ammonium transport.

The pore analysis using HOLE2 did not reveal a continuous solute pathway in the LeAMT1;1 homology model. Most residues, if not all, that have been suggested to be crucial for the NH_4^+ recruitment and NH_3 conduction in the occluded pore of AmtB, are identical or similar in LeAMT1;1. The residues F103, F107, W148 and S219 in AmtB have been predicted to participate in the recruitment and coordination of the NH_4^+ ion; the equivalent residues in LeAMT1;1 are at positions Y133, F137, W178 and S263, respectively. The aromatic residues F107 and F215 block the pore in AmtB, these residues are at positions F137 and F259 in LeAMT1;1. The model has a similar hydrophobic pore to AmtB, with two conserved histidines at positions H207 and H374 that line the putative pore lumen (Fig.1G). Although the model cannot be a substitute for a crystal structure, its similarity to the NH_3 transporting AmtB is striking.

The aromatic nature of two residues forming the ion binding cavity (Y133 and W178 in LeAMT1;1) is conserved between bacterial and plant homologs, but not in Rh glycoproteins. In Rhs, non-polar small neutral residues occupy these positions (Isoleucine and Leucine in RhCG). These residues might thus be responsible for the different affinity that is observed in Rh glycoproteins [7, 8]. The overall quality of the LeAMT1;1 model was tested by mutational analysis of the residues Y133 and W178 that are putatively involved in substrate affinity.

Ammonium transport by LeAMT1;1 pore mutants

Initial attempts to functionally express EcAmtB in oocytes failed *(data not shown)*, so we concentrated on the function of LeAMT1;1. Residues tyrosine 133 and tryptophan 178 were exchanged to the respective residues found in RhC glycoprotein (Y133I and W178L). LeAMT1;1 and, to a lower extent, the two mutants functionally complemented the ammonium-transporter deficient yeast strain ΔΔΔ*mep1,2,3* with ammonium as sole nitrogen source (Fig.2). The mutations did not largely alter the expression pattern as assessed by confocal microscopy of translational c-terminal GFP-fusions in yeast. A similar cell-to-cell variability in fluorescence levels was observed in homogenous yeast cultures when analyzed with the identical microscopy settings at low magnification (Fig.2E). LeAMT1;1 and the mutants showed the same subcellular localization when analyzed at higher magnification (Fig.2E).

125 mM MeA are toxic to wild type yeast and expression of Rh glycoproteins has been shown to rescue growth on toxic MeA. Rh glycoproteins probably export uncharged MeA along its chemical gradient, even though Rh glycoproteins are saturated well below these high MA concentrations [8]. Both mutants and LeAMT1;1 showed increased sensitivity to MeA, which is most simply explained by MeA^+ import by LeAMT1;1 and the mutants (Fig.2D). In all assays, the W178L mutant displayed less transport activity than mutant Y133I.

Altered saturation of NH_4^+ transport in a LeAMT1;1 mutant

For a more detailed analysis, the ionic currents elicited by the mutant transporters were assayed using the two-electrode voltage clamp in oocytes. No significant ^{14}C-MeA uptakes and currents were detected with W178L, precluding further analysis. In contrast, the mutant Y133I displayed small, but reliable currents on exposure to ammonium. Currents were more than 10-fold smaller than in the wild type (Fig.3), in accordance with its reduced overall transport rate or reduced functionality compared to wild type in the yeast growth experiments. Importantly, the half maximal current, which is a measure that is independent of the expression level, saturated at very low concentrations. In contrast to wild type (K_m = 12 μM),

the K_m for NH_4^+ in the Y133I mutant was only 1 μM at –120 mV. Similarly, MeA^+ currents saturated at a half maximal concentration of 584 μM at –120 mV in LeAMT1;1, while the small currents of the mutant were half maximal at 4.5 μM (Fig.3).

Charge coupling of MeA^+ transport in LeAMT1;1

The ratio of charged vs. uncharged solute transport was assayed using the analog methylammonium labeled at its carbon (^{14}C-MeA). Transport and charge translocation were monitored simultaneously in native and LeAMT1;1-expressing oocytes from the same batch. LeAMT1;1-expressing oocytes incubated in 1 mM ^{14}C-MA accumulated 9.0 $\pm$ 1.5 pmol min^{-1} ^{14}C-MeA ($H_3{}^{14}C\text{-}NH_3^+/H_3{}^{14}C\text{-}NH_2$). During incubation, oocytes had a membrane potential of +4 $\pm$ 1 mV. The accumulation rate can be converted using Avogadro's constant into molecules $^x min^{-1}$ of MeA. If each molecule transported is charged ($H_3{}^{14}C\text{-}NH_3^+$ carries one elementary charge), this corresponds to an ionic current of –14.4 $\pm$ 2.4 nA. At the measured resting potential of +4 mV, MeA induced -12.5 nA inward current (Fig.4), suggesting that roughly 100% of MeA is taken up as charged $H_3{}^{14}C\text{-}NH_3^+$. The MeA^+/MeA-induced current was specific to LeAMT1;1-expressing oocytes, was time-independent over several minutes and was strongly inwardly rectifying. Taking the error bar into account, the maximal slippage of uncharged $H_3{}^{14}C\text{-}NH_2$ must be below 10%. Identical results were obtained with 3 independent batches of oocytes; one of these experiments is shown in Fig.4. The results show that preferentially $H_3{}^{14}C\text{-}NH_3^+$ is transported but, at this resolution, the possible transport of $H_3{}^{14}C\text{-}NH_2$ cannot be excluded (Fig.4).

Ionic currents and acidification by LeAMT1;1

To determine if a residual flux of NH_3 is maintained by LeAMT1;1, current and pH_i recordings were combined. Current-voltage relations from LeAMT1;1-expressing oocytes are shown in Fig.5. The open symbols represent a current-voltage relation from LeAMT1;1-expressing oocytes in the absence and the closed circles after addition of 200 μM ammonium (Fig.5A). The ammonium-induced current was inward and the reversal potential of the total currents shifted to more positive membrane potentials. No pH_i changes upon 500 μM ammonium exposure were observed in BCECF–loaded, LeAMT1;1-expressing oocytes and in water-injected controls (Fig.5B). Although NH_4^+ transport is almost saturated by 500 μM in LeAMT1;1 (Fig.3)[5], 10 mM ammonium was also used to compare the results with older studies on native oocytes that used these excess ammonium concentrations. Only negligible NH_4^+ influx is expected from non-voltage clamped, LeAMT1;1-expressing oocytes at depolarized potentials (compare the current-voltage relation in Fig.5A), but significant NH_4^+

influx in voltage-clamped oocytes at a negative membrane potential. The negative membrane potential mimics the *in vivo* situation of LeAMT1;1 in tomato root epidermal cells [22].

The pH_i of water-injected and LeAMT1;1-expressing oocytes clamped to –80 mV is shown in Fig.5C&D. 500 μM ammonium induced –150 nA current in LeAMT1;1 and a persistent acidification, in accordance with NH_4^+ influx, but in opposition to significant NH_3 flux. This acidification was not observed in water-injected control oocytes. It is necessary to recall that at the cytosolic pH_i of 7.4, the pH_i is highly sensitive to NH_3 influx, as almost every incoming NH_3 will bind H^+ to form NH_4^+. This situation is distinct with NH_4^+ transport: most of the influxed NH_4^+ will remain as NH_4^+ and only a minor fraction (~1.5 %) will dissociate into NH_3 and H^+, and thus acidify the cytosol.

The pH_i-changes were not due to possible oocyte to oocyte variability, which is shown in a continuous recording from a single LeAMT1;1-expressing oocyte in Fig.5D. Low ammonium induced acidification and –170 nA current during voltage-clamp, while no acidification was seen when the membrane potential was then allowed to change freely. Interestingly, the voltage-clamped LeAMT1;1 oocytes that acidified with NH_4^+ uptake did not recover the pH_i to the baseline level after the withdrawal of ammonium. This suggests that ammonium that passively exits the oocyte as NH_3, is reabsorbed as NH_4^+ and thus the cytosolic ammonium concentration, and pH_i, are maintained.

Discussion

Prediction of the function of proteins based on their crystal structure is an exceptionally elegant method, but we cannot yet distinguish a channel from a transporter that couples conformational changes to transport on the basis of the crystal structure. The structure of the bacterial AMT/Rh homolog AmtB does not show a clearly open transmembrane pore (Fig.1), which would be required for a channel but is unlikely in any well-coupled exchanger. This is also true for the model of LeAMT1;1, which shows that key residues are highly conserved between these proteins. Thus, even in AmtB, conformational changes or side chain movements are required to allow solute flow. If, however, AmtB undergoes a conformational change that is not detected by the crystallographic approach, then hydrogen bond acceptors may become available for interaction with ammonium.

Similar to the case of AMT/Rh proteins, the X-ray structures of a prokaryotic homolog of CLC anion channels did not reveal its mechanism, which was later identified as rapid $2Cl^-/H^+$ antiport [23]. Although the pathway for anions is well apparent from the atomic CLC-structures, it has not yet been resolved how H^+ is transported in CLCs. Similarly, although

residues involved in sugar/H^+ co-transport in LacY transporters had long been known, the mechanism of H^+ co-transport was not readily apparent from the structure [24]. Crystal structures provide a static view, and even if structures look alike in the presence and absence of substrate, this does not exclude the existence of other conformations, since the protein may preferably crystallize in one state. Solute transport in proteins needs to be viewed as dynamic, but crystallographic structures are, by nature, static. A full understanding of the transport mechanism will only result from a resourceful combination of structural and functional biochemical approaches.

The 3D model of LeAMT1;1 was successfully used to predict residues involved in NH_4^+ recruitment (or binding). Though no attempt is made to derive mechanistic conclusions from the homology model and the hydrophobic pore of LeAMT1;1, the molecular modeling may be useful in guiding future experimental work on this transporter/channel class. A very similar AMT/Rh structure has recently been reported from a thermophilic archaeon [25], which emphasizes that AMT/Rhs adopt a similar structure. The functional data of LeAMT1;1 in Fig.4 and Fig.5 show that LeAMT1;1 is a net NH_4^+ transporter (or "channel"). Based on the AmtB structure and the hydrophobic pore in the LeAMT1;1 model, one may speculate that the molecular mechanism is NH_3/H^+ co-transport. If NH_4^+ dissociates into NH_3 and H^+ during passage, an unresolved pathway would exist for H^+. This had already been discussed [1] and explains the superb selectivity of NH_4^+ transporters against alkali cations [5]. NH_4^+ transport is equal at external pH_o 5.5 and 8.5 [5] and exceeds that of NH_3, which suggests that LeAMT1;1 can transport against NH_3 gradients.

Despite similar key residues in the structure, AmtB apparently uses a different transport mechanism, as it transports at least some NH_3, shown by the rapid alkalinization of AmtB vesicles in ammonium solution [2]. It is currently impossible to exclude the possibility that AmtB is sloppier and passes more NH_3 together with NH_4^+. It remains to be shown that AmtB dissipates NH_3 gradients and thus acts as a channel. Even if AmtB would transport 95% in the form of NH_4^+ and only 5% in the form of NH_3, alkalinization would be expected due to a net inward NH_3 flux (at physiological pH_i total ammonium is ~98.5% NH_4^+ and ~1.5% NH_3).

The data on LeAMT1;1 presented here are in accordance with earlier data [5] and argue against the speculation that LeAMT1;1 currents may be endogenous to oocytes [2]. The saturation of currents was altered by more than 10-fold (NH_4^+) and 100-fold (MeA^+) in LeAMT1;1 mutants and differed from endogenous ammonium-induced oocyte currents [8]. Transport of NH_4^+ is not restricted to LeAMT1;1, since other plant homologs have now been identified in our laboratory which also induce saturable NH_4^+ and MeA^+ currents when

expressed in oocytes [26]. Similar to the plant transporters, the *Saccharomyces* homologs (MEP1-3) are involved in re-uptake and accumulation of lost ammonium [17]. Microorganisms and plants maintain a near neutral cytoplasmic pH_i, but the acidic external pH_o often requires the acquisition of NH_4^+/NH_3 against a NH_3 concentration gradient.

Small conformational changes that may represent "gating" of AmtB have already been documented in the different crystal structures [2, 3], but more structures showing different conformations of AMT/Rhs are required to distinguish between channel and transporter-like mechanisms. In any case, the functional data suggest that the classical concept of clear discrimination between channels and transporters is diminishing on a molecular level: highly similar proteins from the AMT/Rh-family may function as equilibrative "gas" or ion channels/transporters.

Acknowledgements: We thank Binghua Wu for initial help with the constructs, Petra Neumann for excellent technical assistance and Felicity deCourcy for critically reading the manuscript. Support from the Deutsche Forschungsgemeinschaft to U.L is acknowledged.

References

1 Ludewig, U., von Wirén, N., Rentsch, D. and Frommer, W. B. (2001) Rhesus factors and ammonium: a function in efflux? Genome Biol. **2**, 1-5

2 Khademi, S., O'Connell, J., 3rd, Remis, J., Robles-Colmenares, Y., Miercke, L. J. and Stroud, R. M. (2004) Mechanism of ammonia transport by Amt/MEP/Rh: structure of AmtB at 1.35 Å. Science **305**, 1587-1594

3 Zheng, L., Kostrewa, D., Berneche, S., Winkler, F. K. and Li, X. D. (2004) The mechanism of ammonia transport based on the crystal structure of AmtB of Escherichia coli. Proc. Natl. Acad. Sci. U S A **101**, 17090-17095

4 Javelle, A., Thomas, G., Marini, A. M., Kramer, R. and Merrick, M. (2005) In vivo functional characterisation of the E. coli ammonium channel AmtB: evidence for metabolic coupling of AmtB to glutamine synthetase. Biochem J, 215-222

5 Ludewig, U., von Wirén, N. and Frommer, W. B. (2002) Uniport of NH_4^+ by the root hair plasma membrane ammonium transporter LeAMT1;1. J. Biol. Chem. **277**, 13548-13555

6 Ludewig, U., Wilken, S., Wu, B., Jost, W., Obrdlik, P., El Bakkoury, M., Marini, A. M., Andre, B., Hamacher, T., Boles, E., von Wiren, N. and Frommer, W. B. (2003) Homo- and hetero-oligomerization of ammonium transporter-1 NH_4^+ uniporters. J. Biol. Chem. **278**, 45603-45610

7 Ludewig, U. (2004) Electroneutral Ammonium Transport by Basolateral Rhesus B Glycoprotein. J. Physiol. **471**, 751-759

8 Mayer, M., Schaaf, G., Mouro, I., Lopez, C., Colin, Y., Neumann, P., Cartron, J. P. and Ludewig, U. (2006) Different transport mechanism in plant and human AMT/Rh-type ammonium transporters. J Gen Physiol **127**, 133-144

9 Zidi-Yahiaoui, N., Mouro-Chanteloup, I., D'Ambrosio, A. M., Lopez, C., Gane, P., Le van Kim, C., Cartron, J. P., Colin, Y. and Ripoche, P. (2005) Human Rhesus B and Rhesus C glycoproteins: properties of facilitated ammonium transport in recombinant kidney cells. Biochem J. **391**, 33-40

10 Burckhardt, B. C. and Fromter, E. (1992) Pathways of NH_3/NH_4^+ permeation across Xenopus laevis oocyte cell membrane. Pflügers Arch. Eur. J. Physiol. **420**, 83-86

11 Burckhardt, B. C. and Thelen, P. (1995) Effect of primary, secondary and tertiary amines on membrane potential and intracellular pH in Xenopus laevis oocytes. Pflügers Arch. Eur. J. Physiol. **429**, 306-312

12 Holm, L. M., Jahn, T. P., Moller, A. L., Schjoerring, J. K., Ferri, D., Klaerke, D. A. and Zeuthen, T. (2005) NH_3 and NH_4^+ permeability in aquaporin-expressing Xenopus oocytes. Pflugers Arch. Eur. J. Physiol. **450**, 415-428

13 Boldt, M., Burckhardt, G. and Burckhardt, B. C. (2003) NH_4^+ conductance in Xenopus laevis oocytes. III. Effect of NH_3. Pflügers Arch. Eur. J. Physiol. **446**, 652-657

14 Bakouh, N., Benjelloun, F., Hulin, P., Brouillard, F., Edelman, A., Cherif-Zahar, B. and Planelles, G. (2004) NH_3 is involved in the NH_4^+ transport induced by the functional expression of the human RhC glycoprotein. J. Biol. Chem. **279**, 15975-15983

15 Wallner, B. and Elofsson, A. (2005) All are not equal: a benchmark of different homology modeling programs. Protein Sci. **14**, 1315-1327

16 Smart, O. S., Goodfellow, J. M. and Wallace, B. A. (1993) The pore dimensions of gramicidin A. Biophys J **65**, 2455-2460

17 Marini, A. M., Soussi-Boudekou, S., Vissers, S. and André, B. (1997) A family of ammonium transporters in *Saccharomyces cerevisiae*. Mol. Cell. Biol. **17**, 4282-4293

18 Loqué, D., Ludewig, U., Yuan, L. and von Wiren, N. (2005) Tonoplast aquaporins AtTIP2;1 and AtTIP2;3 facilitate NH3 transport into the vacuole. Plant Physiol. **137**, 671-680

19 Jahn, T. P., Moller, A. L., Zeuthen, T., Holm, L. M., Klaerke, D. A., Mohsin, B., Kuhlbrandt, W. and Schjoerring, J. K. (2004) Aquaporin homologues in plants and mammals transport ammonia. FEBS Lett. **574**, 31-36

20 Sui, H., Han, B. G., Lee, J. K., Walian, P. and Jap, B. K. (2001) Structural basis of water-specific transport through the AQP1 water channel. Nature **414**, 872-878

21 Knepper, M. A. and Agre, P. (2004) Structural biology. The atomic architecture of a gas channel. Science **305**, 1573-1574

22 Ayling, S. M. (1993) The effect of ammonium ions on membrane potential and anion flux in roots of barley and tomato. Plant Cell Environ **16**, 297–303

23 Accardi, A. and Miller, C. (2004) Secondary active transport mediated by a prokaryotic homologue of ClC Cl- channels. Nature **427**, 803-807

24 Abramson, J., Iwata, S. and Kaback, H. R. (2004) Lactose permease as a paradigm for membrane transport proteins. Mol. Membr. Biol. **21**, 227-236

25 Andrade, S. L., Dickmanns, A., Ficner, R. and Einsle, O. (2005) Crystal structure of the archaeal ammonium transporter Amt-1 from Archaeoglobus fulgidus. Proc. Natl. Acad. Sci. U S A **102**, 14994-14999

26 Mayer, M. and Ludewig, U. (2006) Role of AMT1;1 in NH4+-acquisition in Arabidopsis thaliana. Plant Biol **8**, in press

Figure legends:

Fig.1: Analysis of the LeAMT1;1 homology model. (A) Ribbon structure of an AmtB monomer backbone (PDB code:1UG7) (B) Structure of the homology model of LeAMT1;1. (C) Upper panel: RMSD from a minimization of the AmtB structure and comparison to the homology model. Lower panel: Pore diameter of AmtB (red) and AQP1 (blue) calculated with the program HOLE2. (D) Pore diameter of the aquaporin AQP1 calculated with HOLE2. (E) Top view of the trimeric assembly of the LeAMT1;1 model. (F) Pore diameter in AmtB. Residues F103, F107, W148 participate in the recruitment (or binding) site for the NH_4^+ ion and F107 and F215 obstruct the pore. The conserved histidine residues His168 and His318 line the hydrophobic pore. Helices M7 and M8 were removed for better visualization. The pore diameters below 0.8 A are shown in red, between 0.8 A and 2.3 A in green, and diameters above 2.3 A are shown in blue. (G) Position of the homologous residues in the model of LeAMT1;1.

Fig.2: Analysis of LeAMT1;1 wild type and NH_4^+ recruitment site mutants (W178L and Y133I) in yeast. Spotted 100-fold dilutions and growth of *ΔΔΔmep1,2,3* strain expressing the respective constructs on limiting ammonium (A) 0,2 mM; (B) 1 mM; (C) 3 mM. (D) Dilution series (10x) of wild type yeast growth expressing the constructs on toxic MeA (125 mM). (E) Expression and subcellular localization of GFP-tagged wild type, Y133I and W178L mutants in yeast; left panel: bright field; right panel: GFP fluorescence. Scaling bars: 5 μm.

Fig.3: Functional analysis of the Y133I mutant in oocytes and comparison with LeAMT1;1 wild type. (A) Saturation of ammonium-induced currents at –120 mV for LeAMT1;1 wild type (open circles, K_m = 12 μM, n=5) and the Y133I mutant (closed triangles, Km = 1 μM, n=9) (B) Same data, but normalized to the same maximal current with a focus on low concentrations. (C) Saturation of MeA-induced currents at –120 mV for wild type (open circles, K_m = 584 μM, n=5) and the Y133I mutant (closed triangles, Km = 4.5 μM, n=5) (D) Same data, but normalized to the same maximal current with a focus on low concentrations.

Fig.4: MeA^+ transport in LeAMT1;1 (A) Induced ionic currents by MeA^+ in LeAMT1;1-expressing oocytes (background currents have been subtracted). The inset magnifies part of the Figure. (B) Uptake of ^{14}C-MeA in LeAMT1;1-expressing oocytes (black bar), not injected

(n.i., grey bar) and LeAMT1;1 mediated (LeAMT1;1 minus n.i., dark grey bar). The uptake of 7.8 pmol*min^{-1} corresponds to 12.5 nA currents measured from the same oocytes (white bar). Constants used for current-charge conversion were: 1 pmol = 6.02*10^{23} particles; elementary charge e^o=1.6*10^{-19}As.

Fig.5: NH_4^+ transport by LeAMT1;1 (A) Ionic currents in oocytes expressing LeAMT1;1 without ammonium (open circles) and with 200 μM NH_4Cl (closed circles). (B) Intracellular pH_i in H_20-injected oocytes (upper trace) and LeAMT1;1 expressing oocytes (lower trace) by 1 mM MeA, 500 μM ammonium and alkalinization by 10 mM ammonium. Note the pH_i overshoot by 10 mM ammonium in LeAMT1;1 oocytes. (C) As in B, but cytosolic pH_i in voltage clamped oocytes (to –80 mV) (D) Representative pH_i trace from a LeAMT1;1 expressing oocyte at –80 mV, then not voltage clamped, and again clamped to –80 mV. Alkalinization is shown as upward and acidification as downward deflection throughout the figure.

Biochemical Journal Immediate Publication. Published on 27 Feb 2006 as manuscript BJ20060051

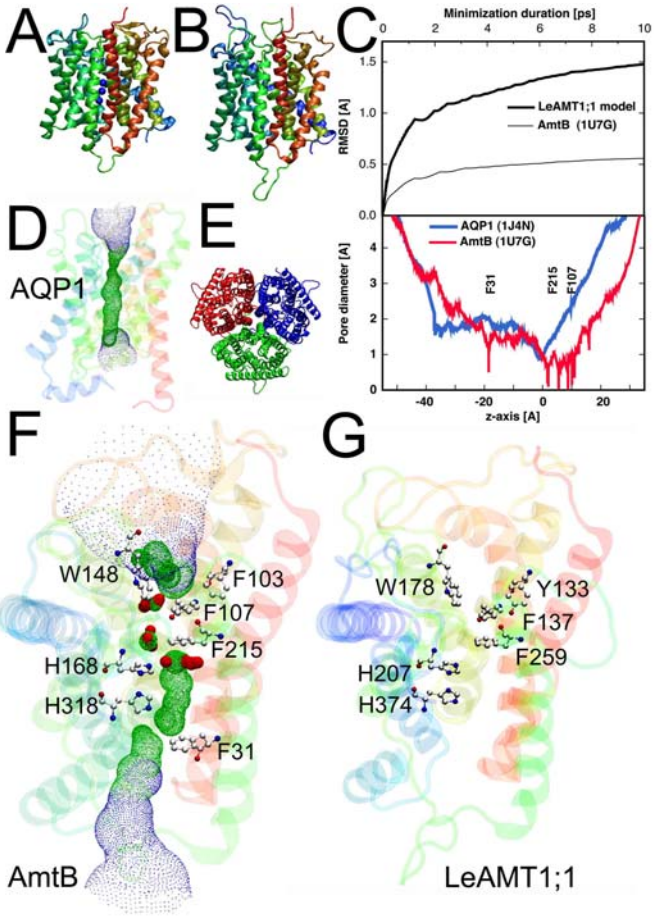

Biochemical Journal Immediate Publication. Published on 27 Feb 2006 as manuscript BJ20060051

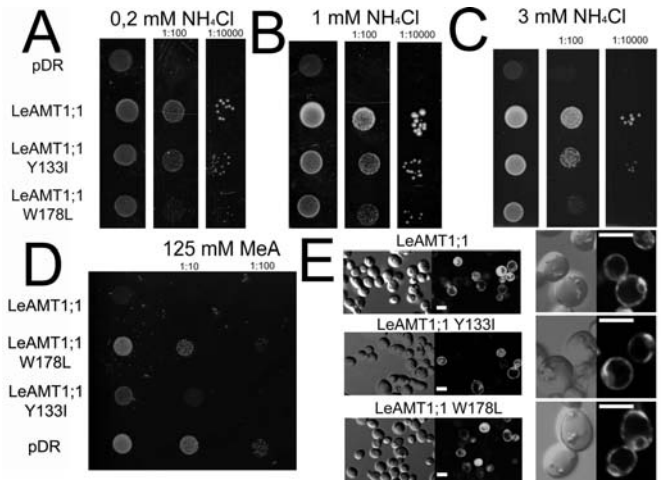

Biochemical Journal Immediate Publication. Published on 27 Feb 2006 as manuscript BJ20060051

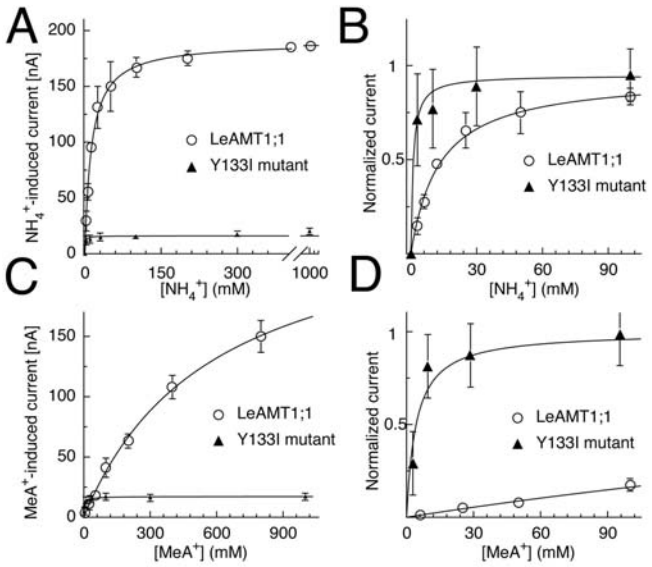

Biochemical Journal Immediate Publication. Published on 27 Feb 2006 as manuscript BJ20060051

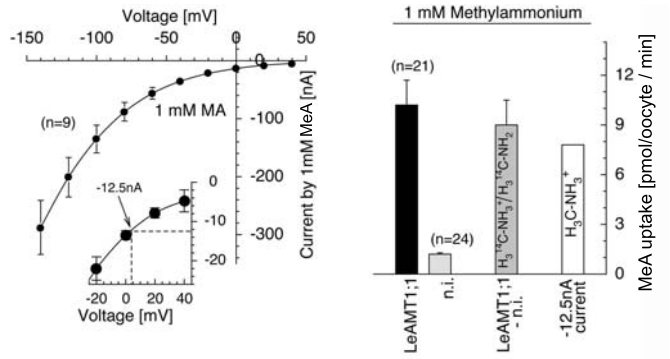

Biochemical Journal Immediate Publication. Published on 27 Feb 2006 as manuscript BJ20060051